

## Research Paper

# Pilot Prospective Evaluation of $^{18}\text{F}$ -Alfatide II for Detection of Skeletal Metastases

Baoming Mi<sup>1#</sup>, Chunjing Yu<sup>1#</sup>, Donghui Pan<sup>2</sup>, Min Yang<sup>2✉</sup>, Weixing Wan<sup>1✉</sup>, Gang Niu<sup>3✉</sup>, Xiaoyuan Chen<sup>3✉</sup>

1. Department of Nuclear Medicine, Affiliated Hospital of Jiangnan University (Wuxi 4<sup>th</sup> People's Hospital), Wuxi, China
2. Key Laboratory of Nuclear Medicine, Ministry of Health, Jiangsu Key Laboratory of Molecular Nuclear Medicine, Jiangsu Institute of Nuclear Medicine, Wuxi, China
3. Laboratory of Molecular Imaging and Nanomedicine, National Institute of Biomedical Imaging and Bioengineering, National Institutes of Health, Bethesda, MD, USA

#Contributed equally to this work

✉ Corresponding authors: Weixing Wan (wwwxs@126.com); Min Yang (ymzfk@yahoo.com.hk); Gang Niu (niug@mail.nih.gov); Xiaoyuan Chen (shawn.chen@nih.gov)

© 2015 Ivyspring International Publisher. Reproduction is permitted for personal, noncommercial use, provided that the article is in whole, unmodified, and properly cited. See <http://ivyspring.com/terms> for terms and conditions.

Received: 2015.06.11; Accepted: 2015.07.01; Published: 2015.07.12

## Abstract

This pilot prospective evaluation study is to verify the efficiency of  $^{18}\text{F}$ -Alfatide II, a specific PET imaging agent for integrin  $\alpha\beta_3$ , in detecting bone metastasis in human, with comparison to  $^{18}\text{F}$ -FDG PET. Thirty recruited patients underwent  $^{18}\text{F}$ -FDG and  $^{18}\text{F}$ -alfatide II PET/CT successively within days. The final diagnosis of bone lesions was established based on the comprehensive assessment of all available data and clinical follow-up, which fall into four groups: osteolytic, osteoblastic, mixed and bone marrow. Visual analysis and quantification of  $\text{SUV}_{\text{max}}$  were performed to compare the detection sensitivity of  $^{18}\text{F}$ -Alfatide II and  $^{18}\text{F}$ -FDG PET. Eleven patients were found to have a total of 126 bone metastasis lesions.  $^{18}\text{F}$ -Alfatide II PET can detect the bone metastatic lesions with good contrast and higher sensitivity (positive rate of 92%) than  $^{18}\text{F}$ -FDG PET (77%). Especially,  $^{18}\text{F}$ -Alfatide II PET showed superiority to  $^{18}\text{F}$ -FDG PET in detecting osteoblastic (70% vs. 53%) and bone marrow metastatic lesions (98% vs. 77%). In conclusion,  $^{18}\text{F}$ -Alfatide II PET/CT can be used to detect skeletal and bone marrow metastases, with nearly 100% sensitivity in osteolytic, mixed and bone marrow lesions. The sensitivity of  $^{18}\text{F}$ -Alfatide II PET/CT in osteoblastic metastases is relatively low but still significantly higher than that of  $^{18}\text{F}$ -FDG PET/CT. This pilot clinical study warrants the further application of  $^{18}\text{F}$ -Alfatide II PET/CT in metastatic lesion detection, patient management and drug therapy response monitoring.

Key words: RGD peptide; Alfatide II; FDG; PET/CT; bone metastasis

## INTRODUCTION

Skeletal and bone marrow metastases occur mainly in patients with primary breast, prostate, or lung cancer [1]. Early detection of skeletal metastases can significantly change the staging of the disease, alter the treatment strategy and decrease the morbidity. Several imaging modalities, including X-ray, computed tomography (CT), magnetic resonance imaging (MRI),  $^{99\text{m}}\text{Tc}$ -MDP (methylenediphosphonic

acid) bone scan, and  $^{18}\text{F}$ -FDG PET have been adopted to detect bone metastasis [2].  $^{99\text{m}}\text{Tc}$ -MDP bone scan remains to be the mainstay of evaluating skeletal metastasis, due to its sensitivity in visualizing both osteolytic and osteoblastic bone metastases on whole-body images at reasonable cost [3]. The bone scan often needs to be followed by either CT or MRI to depict anatomic changes in more details [4].

With the increased availability of PET/CT, FDG scan is commonly performed for cancer detection and staging, as it can detect metastatic disease in multiple organ systems [5]. Consequently, the application of FDG PET/CT to detect skeletal metastatic disease has been intensively investigated. Most reports suggest that FDG PET/CT is superior to bone scan in the detection of skeletal metastatic disease [6, 7]. Similar to the primary lesion, visualization of bone metastasis by FDG PET/CT is also based on the increased metabolic activity rather than anatomical alterations. It is well known that  $^{18}\text{F}$ -FDG is not highly specific in differentiating malignancy and inflammation. In addition, some types of malignancies such as prostate cancer usually do not have high glucose uptake and are not readily diagnosed by FDG PET [8]. Therefore, there is still a need to explore other imaging probes to provide more information of bone metastases for individualized diagnosis and treatment.

Integrin  $\alpha_v\beta_3$  is involved in the interaction of endothelial cells and extracellular matrix during tumor-induced formation of new vessels as well as in mediation of tumor cell migration during invasion and extravasation [9, 10]. Consequently, a variety of radioactive tracers based on RGD (Arginine-glycine-aspartic acid) peptides have been developed for noninvasive determination of  $\alpha_v\beta_3$  expression [11-16]. Several of these tracers labeled either with  $^{68}\text{Ga}$  or  $^{18}\text{F}$  are currently in clinical trials, including  $^{18}\text{F}$ -Galacto-RGD [11],  $^{18}\text{F}$ -alfatide [13],  $^{68}\text{Ga}$ -RGD [17] and  $^{18}\text{F}$ -FPPRGD2 [18]. All these studies confirmed the feasibility and diagnostic value of integrin  $\alpha_v\beta_3$  targeted PET imaging. In addition, increased tracer uptake has been found in bone metastases [19, 20].

Our previous studies showed that  $^{18}\text{F}$ -Alfatide can be produced with excellent radiochemical yield and purity *via* a simple one-step lyophilized kit. PET with  $^{18}\text{F}$ -alfatide allowed specific imaging of  $\alpha_v\beta_3$  expression with excellent imaging contrast in humans [13]. To further improve the tracer stability and imaging quality, we developed a new tracer  $^{18}\text{F}$ -NOTA-E[PEG4-c(RGDfk)]<sub>2</sub> (denoted as Alfatide II) [21, 22]. In this study, we performed a clinical investigation, aiming to verify the detection efficiency of  $^{18}\text{F}$ -Alfatide II PET in different types of bone metastases including osteolytic, osteoblastic, mixed and bone marrow metastases, in comparison with  $^{18}\text{F}$ -FDG PET.

## MATERIALS AND METHODS

### Patient Recruitment

The study protocol was approved by the ethics committee of the Affiliated Hospital of Jiangnan

University (Wuxi 4th People's Hospital) and registered at ClinicalTrials.gov (NCT02441972). Thirty patients were recruited after their routine  $^{18}\text{F}$ -FDG PET/CT examination, and each patient gave written and informed consent before the  $^{18}\text{F}$ -Alfatide II PET/CT study. The final diagnosis of bone lesions was established based on the comprehensive assessment of all available data and clinical follow up.

### PET/CT Protocol

The standard protocol for an  $^{18}\text{F}$ -FDG PET/CT scan was adopted. Patients were asked to fast for 4-6 h immediately before the scan. An  $^{18}\text{F}$ -FDG dose of  $10 \pm 1.5$  mCi ( $370 \pm 55.5$  MBq) was intravenously administered. At 1 h after injection, the patients were scanned on a Siemens TruePoint HD scanner.  $^{18}\text{F}$ -Alfatide II PET was performed within 1 to 3 days after the  $^{18}\text{F}$ -FDG PET. No patient preparation was required for the  $^{18}\text{F}$ -Alfatide II PET scan. The injection dose of  $^{18}\text{F}$ -Alfatide II was  $8 \pm 1.0$  mCi ( $296 \pm 37$  MBq). At 1 h after injection, the patients were scanned on the same Siemens TruePoint HD scanner. For both radiopharmaceuticals, whole-body (vertex to thigh) PET/CT images were obtained in 3D mode (2 min per bed position). Low-dose helical CT transmission scan (pitch 0.8, 50 mAs, 120 kV (peak)) was performed first for each of the 2 scans. Raw CT data were reconstructed into 3.75 mm-thick sections of transverse images, and reformatted sagittal and coronal CT images were generated. CT-based attenuation-corrected PET images were reconstructed with a standard iterative algorithm (OSEM, 3 iterative steps, 21 subsets) and reviewed using the same Siemens MMWP workstation.

### Image Analysis

$^{18}\text{F}$ -FDG PET and  $^{18}\text{F}$ -Alfatide II PET images were scored according to the visual analysis on a per-lesion basis by two independent board-certified nuclear medicine physicians, who were unaware of the final diagnosis and the results of the other imaging studies. A 4-point grade system was adopted to describe the uptake degree for bone lesions: grade 0, uptake similar to the surrounding bone structure; grade 1, slightly higher uptake than the surrounding bone structure; grade 2, significantly higher uptake than the surrounding bone structure; and grade 3, abnormal concentrated uptake. Lesions scored as grade 0 were taken as negative lesions and those with a score equal to or greater than grade 1 were taken as positive lesions.

The final diagnosis was based on clinical follow-up and imaging results with the specific standards as follows: no history of trauma within half a year, no bone inflammatory disease such as tubercu-

**Table 1.** Patient demographics

Patient no.	Age (y)	Sex	Histology	Different types of bone metastases (number)			
				Osteolytic	Osteoblastic	Mixed	Bone marrow
1	68	F	lung cancer	14	0	0	8
2	66	M	metastatic adenocarcinoma of unknown primary site	4	0	1	7
3	39	M	metastatic adenocarcinoma of unknown primary site	2	6	17	7
4	75	M	lung cancer	0	0	1	3
5	70	M	urinary bladder cancer and gastric cancer	2	4	2	0
6	68	F	lung cancer	1	0	0	12
7	48	M	lung cancer	0	18	0	3
8	81	M	lung cancer	0	2	0	3
9	52	F	lung cancer	3	0	0	0
10	72	F	lung cancer	4	0	0	1
11	59	M	gastric cancer	1	0	0	0

losis and sarcoidosis, no bone fracture and bone tuberculosis. Bone metastasis was diagnosed by meeting either of the following criteria: a score equals to or greater than grade 2 on either  $^{18}\text{F}$ -FDG and/or  $^{18}\text{F}$ -Alfatide II PET, a score equals to grade 1 on both  $^{18}\text{F}$ -FDG and  $^{18}\text{F}$ -Alfatide II PET, or a lesion confirmed on  $^{99\text{m}}\text{Tc}$ -MDP bone scan, X-ray, CT (including the corresponding CT of PET/CT) or MRI examination. The osteolytic, osteoblastic, mixed bone metastatic lesions were classified based on CT characteristics. Bone marrow metastatic lesions were recognized as lesions with abnormal uptake of  $^{18}\text{F}$ -FDG or  $^{18}\text{F}$ -alfatide II in tubular bone marrow cavity or located in the skeletal system but without CT changes.

### Statistical Analysis

Data were expressed as mean  $\pm$  SD. K statistic was used to determine inter-reader agreement for visual analysis. The McNemar test was used to compare  $^{18}\text{F}$ -FDG and  $^{18}\text{F}$ -Alfatide II PET/CT with respect to sensitivity of the two methods. Diagnostic values for bone lesion detection were calculated on a per-lesion basis. For all statistical analyses, a p value  $<0.05$  was considered statistically significant.

## RESULTS

### Diagnosis of Bone Metastases

Twenty-five out of the 30 recruited patients were diagnosed to have malignancies (Table 1). Eleven of them were confirmed to have metastatic bone lesions according to the standard described above. Among these 11 patients, 7 patients had lung cancer, 1 patient had gastric cancer, 1 patient had urinary bladder cancer associated with gastric cancer, and 2 patients had metastatic adenocarcinoma with unknown primary sites. Within the 11 patients, a total of 126 bone metastatic lesions were eventually identified.

### Detection of Metastatic Bone Lesions by $^{18}\text{F}$ -Alfatide II PET

Normally, the highest activity of  $^{18}\text{F}$ -Alfatide II was found in the kidneys and bladder, demonstrating predominant renal clearance of the tracer. Liver, spleen, and intestines also showed moderate uptake, while normal bone and bone marrow had very low background level of radioactivity distribution. Therefore,  $^{18}\text{F}$ -Alfatide II PET has the potential to visualize bone metastatic lesions with high contrast to surrounding background (Figure 1).

In order to compare the diagnostic value of  $^{18}\text{F}$ -Alfatide II PET and  $^{18}\text{F}$ -FDG PET, each bone metastatic lesion was scored based on the standard of visual analysis described previously. Among the 126 bone metastatic lesions, 57 of which were graded equally on both  $^{18}\text{F}$ -Alfatide II PET and  $^{18}\text{F}$ -FDG PET, 43 lesions were graded higher on  $^{18}\text{F}$ -Alfatide II and 26 were graded higher on  $^{18}\text{F}$ -FDG PET (Table 2).

**Table 2.** Visual analysis of metastatic bone lesions based on  $^{18}\text{F}$ -Alfatide II and  $^{18}\text{F}$ -FDG PET

Grade	$^{18}\text{F}$ -Alfatide II PET	$^{18}\text{F}$ -FDG PET
0	10	29
1	32	32
2	51	26
3	33	39

Based on the image characteristics on CT scans, these bone metastatic lesion were further divided into four categories including the osteolytic, osteoblastic, mixed and bone marrow. Both  $^{18}\text{F}$ -Alfatide II and  $^{18}\text{F}$ -FDG showed uptake in these lesions with varied intensity. In some cases,  $^{18}\text{F}$ -Alfatide II showed higher local accumulation than  $^{18}\text{F}$ -FDG, especially in cases of bone marrow metastases (Figure 2 and Figure 3). For all 126 lesions,  $^{18}\text{F}$ -Alfatide II PET showed higher positive rate than  $^{18}\text{F}$ -FDG PET (92% vs. 77%, Table 3). Especially, all osteolytic and mixed bone metastases

were detected by <sup>18</sup>F-Alfatide II PET with a sensitivity rate of 100%. <sup>18</sup>F-Alfatide II PET was also very sensitive in detection of bone marrow lesions with a sensitivity of 98%, which is significantly higher than <sup>18</sup>F-FDG PET (77%). <sup>18</sup>F-Alfatide II PET was not so sensitive in detection of osteoblastic lesions but still with a significantly higher detection rate than <sup>18</sup>F-FDG PET (70% vs. 53%).

**Table 3.** Categorization of the metastatic bone lesions by <sup>18</sup>F-Alfatide II and <sup>18</sup>F-FDG PET

Lesions	<sup>18</sup> F-Alfatide II	<sup>18</sup> F-FDG
Osteolytic (31)	31 (100%)	28 (90%)
Osteoblastic (30)	21 (70%)	16 (53%)
Mixed (21)	21 (100%)	19 (90%)
Bone marrow (44)	43 (98%)	34 (77%)
Total (126)	116 (92%)	97 (77%)

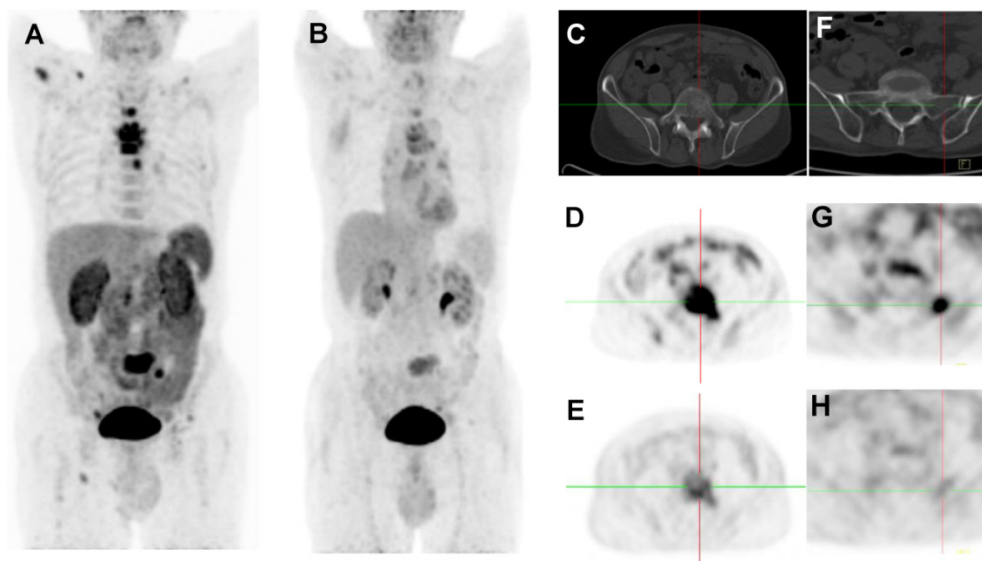


**Figure 1.** 2D projection images of <sup>18</sup>F-Alfatide II PET (A) and <sup>18</sup>F-FDG PET (B) of a patient (no. 2) with metastatic adenocarcinoma of unknown primary site. <sup>18</sup>F-Alfatide II PET demonstrated intense local accumulation of radioactivity in bone metastatic lesions located in thoracic vertebrae, sacrum and right scapula, and right clavicle with good background contrast, whereas <sup>18</sup>F-FDG PET only showed moderate uptake in some thoracic vertebrae and sacral lesions. The transaxial CT (C), <sup>18</sup>F-Alfatide II PET (D), and <sup>18</sup>F-FDG PET (E) were presented to focus on the lesions at sacrum. There is also bone metastasis with abnormal <sup>18</sup>F-Alfatide II uptake (G) but not visible by transaxial CT (F) or <sup>18</sup>F-FDG PET (H).

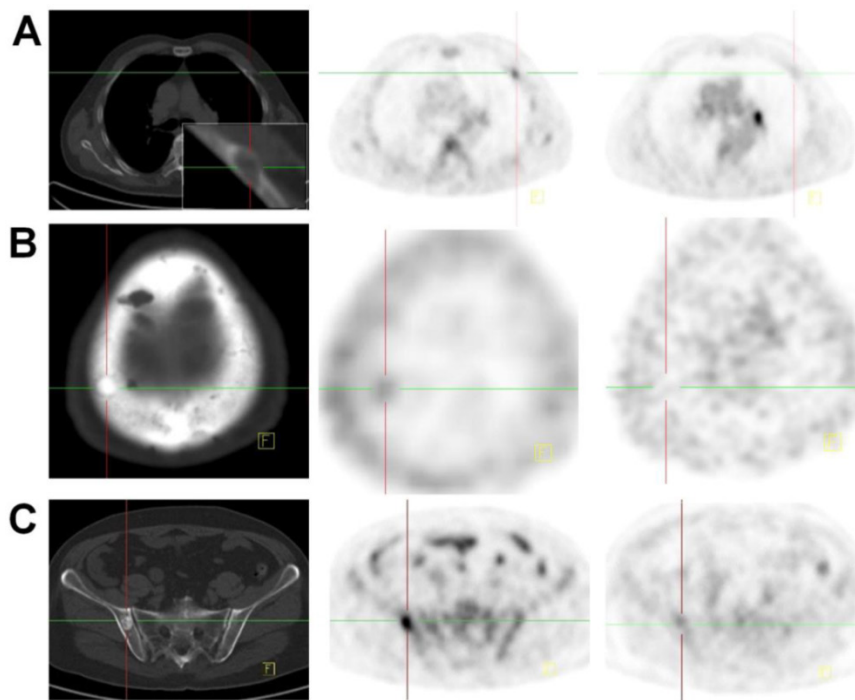


**Figure 2.** CT (left), <sup>18</sup>F-Alfatide II PET (middle), and <sup>18</sup>F-FDG PET (right) of a patient (no. 5) with bladder cancer for 9 years and newly diagnosed with gastric cancer. A lesion in sinuses ventriculi with high FDG uptake was confirmed as adenocarcinoma by biopsy. Multiple metastatic bone lesions were confirmed either as osteolytic (A), osteoblastic (B) or mixed (C) by CT. These lesions showed low or no uptake on <sup>18</sup>F-FDG PET and accumulation of <sup>18</sup>F-Alfatide II with various intensities.



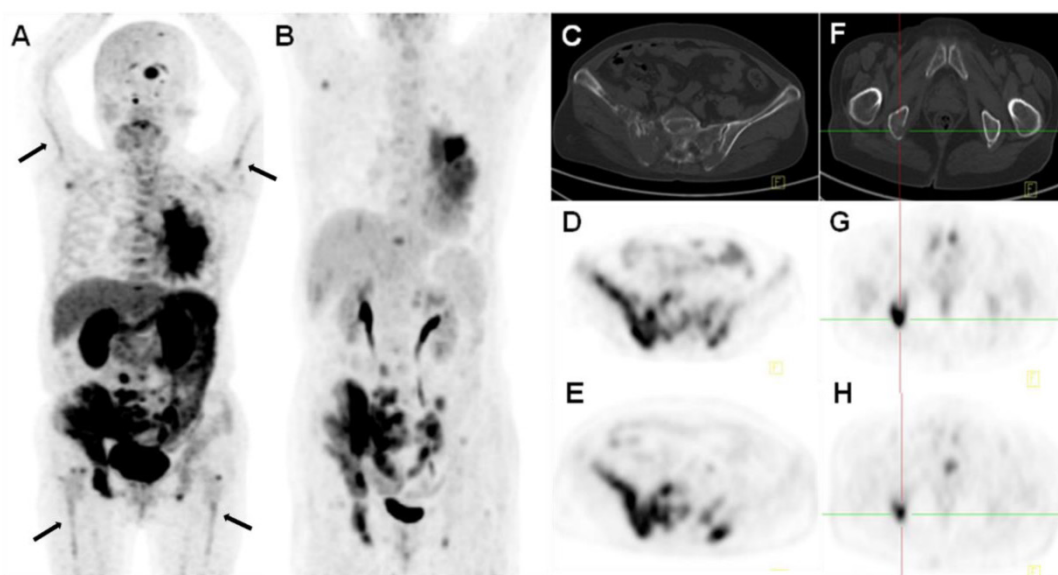


**Figure 3.**  $^{18}\text{F}$ -Alfatide II PET (A, D, E) and  $^{18}\text{F}$ -FDG PET (B, G, H) of a 68-y-old female patient (no. 1) with lung cancer. Besides the primary tumor in the left lung and multiple vertebral osteolytic bone metastases (C, F), bilateral humerus and femur bone marrow cavities showed strip-shaped radiotracer uptake on  $^{18}\text{F}$ -Alfatide II PET.  $^{18}\text{F}$ -FDG PET only discerned the primary site and bone metastases, but not the abnormality in the bone marrow cavities.

### Quantification of Tracer Uptake in Bone Lesions

Both tracers showed relatively large variance in tracer uptake in bone lesions with a range from 0.6 to 11.91 for  $^{18}\text{F}$ -FDG and 0.95 to 13.87 for  $^{18}\text{F}$ -Alfatide II (Figure 4). In all groups, no significant difference was found between  $^{18}\text{F}$ -FDG and  $^{18}\text{F}$ -Alfatide II ( $P > 0.05$  for all comparisons). Both tracers showed significantly lower accumulation in osteoblastic lesions than that in osteolytic and mixed lesions ( $P < 0.001$  for all comparisons).  $\text{SUV}_{\text{max}}$  of  $^{18}\text{F}$ -FDG in osteoblastic lesions was also significantly lower than that in bone marrow metastases ( $P < 0.05$ ). However, there was no significant difference of  $^{18}\text{F}$ -Alfatide II  $\text{SUV}_{\text{max}}$  in osteoblastic lesions and bone marrow metastases.

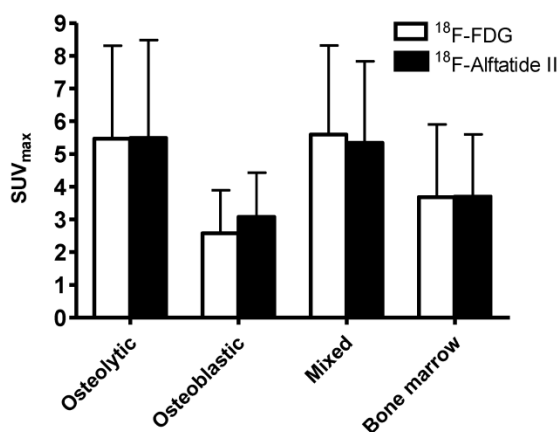


**Figure 4.**  $\text{SUV}_{\text{max}}$  of  $^{18}\text{F}$ -FDG and  $^{18}\text{F}$ -Alfatide II PET in different categories of bone metastases.

### DISCUSSION

In this study, we demonstrated the efficacy of  $^{18}\text{F}$ -Alfatide II PET in detecting metastatic bone diseases. The rationale of this investigation was based on the overexpression of integrin  $\alpha_v\beta_3$  on many types of malignant cells, endothelial cells of tumor vasculature [9], as well as mature osteoclasts [23, 24]. Moreover, the receptor is not expressed or expressed at a very low level on the quiescent endothelium and other normal tissues. The preclinical data also supported that RGD-based PET tracer has the potential to effectively image osteolytic bone metastases [25]. As a specific radiopharmaceutical for integrin  $\alpha_v\beta_3$ ,  $^{18}\text{F}$ -Alfatide II demonstrated high accumulation in various metastatic bone lesions with high lesion-to-background contrast.

Bone metastases are typically characterized as 'osteolytic', 'osseous' or 'mixed', according to the radiographic and/or pathologic major appearance of the lesions [26]. Compared with bone scan,  $^{18}\text{F}$ -FDG PET/CT showed higher sensitivity for detecting osteolytic and mixed bone metastases [6, 27]. Our results demonstrated that  $^{18}\text{F}$ -Alfatide II PET/CT had similar detection efficiency as  $^{18}\text{F}$ -FDG PET/CT for the detection of osteolytic and mixed bone metastases. Moreover,  $^{18}\text{F}$ -Alfatide II PET/CT was superior to  $^{18}\text{F}$ -FDG PET/CT for detecting osseous lesions, especially for the osteoblastic lesions. This phenomenon has not been discovered in preclinical studies due to the limited availability of osseous bone metastasis animal models [25, 28].

In osteoblastic metastatic sites, local stimulation of osteoblast activity results in bone formation directly adjacent to the metastatic tumor. Consequently, a lot of osteoclasts exist in these lesions [29]. It is reasonable to speculate that visualization of bone metastases by  $^{18}\text{F}$ -Alfatide II PET is a result of binding of RGD peptide to integrin  $\alpha_v\beta_3$  expressed on the metastatic tumor cells, endothelial cells and osteoclasts. On the other hand, only metastatic tumor cells with high rate of glycolysis but not endothelial cells or osteoclasts have preferred accumulation of  $^{18}\text{F}$ -FDG [30]. The osteoblastic lesions are often undiscerned on  $^{18}\text{F}$ -FDG PET, because such lesions contain relatively few tumor cells.

Bone marrow (BM) infiltration is the first step of bone metastasis of cancer cells survived the rigors of the systemic circulation [29]. Biopsy of BM, the "gold standard" [31], can miss the focal infiltration, leading to false negative results and negatively affecting clinical management [32]. Recently,  $^{18}\text{F}$ -FDG PET has been applied for BM metastasis detection and FDG-PET/CT appears to have more accurate diagnosis than CT in early detection of BM metastasis [33]. For bone marrow metastatic lesions, the positive rate of  $^{18}\text{F}$ -Alfatide II PET was also higher than that of  $^{18}\text{F}$ -FDG PET (98% *vs.* 77%). The reason may lie in either subclonal selection of integrin  $\alpha_v\beta_3$ -expressing tumor cell populations or upregulation of integrin  $\alpha_v\beta_3$  in the bone microenvironment during the early phase of bone metastasis [34].

It has been reported previously that the sensitivity for various primary and metastatic cancer lesion detection was significantly higher for  $^{18}\text{F}$ -FDG PET compared with that for  $^{18}\text{F}$ -galacto-RGD PET [20]. In this study of bone metastatic lesions, no significant difference in tracer uptake was observed between  $^{18}\text{F}$ -Alfatide II and  $^{18}\text{F}$ -FDG ( $4.27 \pm 2.42$  *vs.*  $4.18 \pm 2.58$ ,  $P > 0.05$ ). There are two possible reasons accounting for this observation: One is that Alfatide II is a dimeric RGD peptide, which has much higher integrin binding affinity than the galacto-RGD monomer. The other reason lies in that only bone metastasis cases were included in this study. The abundance of osteoclasts in these lesions was partially responsible for the high Alfatide II accumulation as the osteoclasts express high level of integrin  $\alpha_v\beta_3$  [23].

Several limitations exist in this study. First, our study lacks histologic verification for the imaging findings because it is not ethical to perform biopsy on patients diagnosed with bone metastasis. Instead, we used a combination of follow-up imaging and clinical management data to verify PET/CT findings, which has commonly been used in previous clinical studies [6]. Second, no comparison with bone scans using either  $^{99\text{m}}\text{Tc}$ -MDP or  $^{18}\text{F}$ -NaF [35] was made. It has

been shown that  $^{99\text{m}}\text{Tc}$ -3PRGD2, a SPECT probe targeting integrin  $\alpha_v\beta_3$ , was efficient in detecting bone metastases when compared with  $^{99\text{m}}\text{Tc}$ -MDP bone scan [36]. In view of the higher sensitivity of PET over SPECT, we believe that  $^{18}\text{F}$ -Alfatide II PET/CT should be superior to  $^{99\text{m}}\text{Tc}$ -MDP bone scan, although a direct comparison study may be needed. It has been reported previously that  $^{18}\text{F}$ -NaF PET is more effective than both planar bone scan and SPECT for bone metastasis detection [35]. Instead of reflecting bone metabolic activity directly,  $^{18}\text{F}$ -Alfatide II PET/CT is more related to integrin  $\alpha_v\beta_3$  upregulation within the microenvironment of bone metastasis. Third, due to the limited number of enrolled patients and heterogeneity of the primary tumors, the number of lesions of each type of cancer was relatively small. In addition, about 30% of lesions were classified as the "bone marrow" metastases group since no obvious osteolytic or osteoblastic changes were shown in the early stage of metastasis. Therefore, further investigation of the detection efficiency of different lesions from different types of cancer is needed, especially for those from breast cancer (mainly osteolytic bone metastases) and prostate cancer (mainly osteoblastic bone metastases).

## CONCLUSION

$^{18}\text{F}$ -Alfatide II PET/CT showed high positive predictive value in the detection of bone metastases, especially in osteolytic, mixed bone and bone marrow metastases. It is of modest sensitivity in detection of osteoblastic lesions but still with a significantly higher detection rate than  $^{18}\text{F}$ -FDG PET. This pilot study encourages further investigation of  $^{18}\text{F}$ -Alfatide II PET/CT in metastatic lesion detection, patient management and drug therapy response monitoring.

## ACKNOWLEDGMENT

This work was supported in part, by the National Basic Research Program of China (973 program, 2013CB733802, 2014CB744503), National Natural Science Foundation (81028009, 81171399, 51473071, 81472749, 81401450, 81471691), National Significant New Drugs Creation Program (2012ZX09505-001-001), Jiangsu Province Foundation (BE2012622, BL2012031, BM2012066, BE2014609), Outstanding Professional Fund of Health Ministry in Jiangsu Province (RC2011095, Q201406), Wuxi Hospital Management Center Project (YGZXM14026, YGZXL1316), and Intramural Research Program of the National Institute of Biomedical Imaging and Bioengineering (NIBIB), National Institutes of Health (NIH).

## COMPETING INTERESTS

The authors have declared that no competing interest exists.

## REFERENCES

- Coleman RE. Clinical features of metastatic bone disease and risk of skeletal morbidity. *Clin Cancer Res.* 2006; 12: 6243s-9s. doi:10.1158/1078-0432.CCR-06-0931.
- Hamaoka T, Madewell JE, Podoloff DA, Hortobagyi GN, Ueno NT. Bone imaging in metastatic breast cancer. *J Clin Oncol.* 2004; 22: 2942-53. doi:10.1200/JCO.2004.08.181.
- Costelloe CM, Rohren EM, Madewell JE, Hamaoka T, Theriault RL, Yu TK, et al. Imaging bone metastases in breast cancer: techniques and recommendations for diagnosis. *Lancet Oncol.* 2009; 10: 606-14. doi:10.1016/S1470-2045(09)70088-9.
- Schmidt GP, Schoenberg SO, Reiser MF, Baur-Melnyk A. Whole-body MR imaging of bone marrow. *Eur J Radiol.* 2005; 55: 33-40. doi:10.1016/j.ejrad.2005.01.019.
- Lewis P, Griffin S, Marsden P, Gee T, Nunan T, Malsey M, et al. Whole-body <sup>18</sup>F-fluorodeoxyglucose positron emission tomography in preoperative evaluation of lung cancer. *Lancet.* 1994; 344: 1265-6.
- Chang CY, Gill CM, Joseph Simeone F, Taneja AK, Huang AJ, Torriani M, et al. Comparison of the diagnostic accuracy of <sup>99m</sup>Tc-MDP bone scintigraphy and <sup>18</sup>F-FDG PET/CT for the detection of skeletal metastases. *Acta Radiol.* 2014. doi:10.1177/0284185114564438.
- Ozulkar T, Kucukoz Uzun A, Ozulkar F, Ozpacac T. Comparison of <sup>18</sup>F-FDG-PET/CT with <sup>99m</sup>Tc-MDP bone scintigraphy for the detection of bone metastases in cancer patients. *Nucl Med Commun.* 2010; 31: 597-603. doi:10.1097/MNM.0b013e328388e909.
- Rohren EM, Turkington TG, Coleman RE. Clinical applications of PET in oncology. *Radiology.* 2004; 231: 305-32. doi:10.1148/radiol.2312021185.
- Niu G, Chen X. Why integrin as a primary target for imaging and therapy. *Theranostics.* 2011; 1: 30-47.
- Brooks PC, Clark RA, Cheresh DA. Requirement of vascular integrin  $\alpha v \beta 3$  for angiogenesis. *Science.* 1994; 264: 569-71.
- Beer AJ, Grosu AL, Carlsen J, Kolk A, Sarbia M, Stangier I, et al. [<sup>18</sup>F]galacto-RGD positron emission tomography for imaging of  $\alpha v \beta 3$  expression on the neovasculature in patients with squamous cell carcinoma of the head and neck. *Clin Cancer Res.* 2007; 13: 6610-6.
- Guo N, Lang L, Li W, Kiesewetter DO, Gao H, Niu G, et al. Quantitative analysis and comparison study of [<sup>18</sup>F]AIF-NOTA-PRGD2, [<sup>18</sup>F]FPPRGD2 and [<sup>68</sup>Ga]Ga-NOTA-PRGD2 using a reference tissue model. *PLoS One.* 2012; 7: e37506. doi:10.1371/journal.pone.0037506.
- Liu D, Wang Z, Jin A, Huang X, Sun X, Wang F, et al. Acetylcholinesterase-catalyzed hydrolysis allows ultrasensitive detection of pathogens with the naked eye. *Angew Chem Int Ed Engl.* 2013; 52: 14065-9. doi:10.1002/anie.201307952.
- Zhou Y, Chakraborty S, Liu S. Radiolabeled Cyclic RGD Peptides as Radiotracers for Imaging Tumors and Thrombosis by SPECT. *Theranostics.* 2011; 1: 58-82.
- Chen X, Hou Y, Tohme M, Park R, Khankaldyyan V, Gonzales-Gomez I, et al. Pegylated Arg-Gly-Asp peptide: <sup>64</sup>Cu labeling and PET imaging of brain tumor  $\alpha v \beta 3$ -integrin expression. *J Nucl Med.* 2004; 45: 1776-83.
- Chen X, Park R, Shahinian AH, Tohme M, Khankaldyyan V, Bozorgzadeh MH, et al. <sup>18</sup>F-labeled RGD peptide: initial evaluation for imaging brain tumor angiogenesis. *Nucl Med Biol.* 2004; 31: 179-89. doi:10.1016/j.nucmedbio.2003.10.002.
- Choi H, Phi JH, Paeng JC, Kim SK, Lee YS, Jeong JM, et al. Imaging of integrin  $\alpha v \beta 3$  expression using <sup>68</sup>Ga-RGD positron emission tomography in pediatric cerebral infarct. *Mol Imaging.* 2013; 12: 213-7.
- Withofs N, Signolle N, Somja J, Lovinfosse P, Mutijima Nzaramba E, Mievies F, et al. <sup>18</sup>F-FPPRGD2 PET/CT imaging of integrin  $\alpha v \beta 3$  in renal carcinomas: Correlation with histopathology. *J Nucl Med.* 2015. doi:10.2967/jnumed.114.149021.
- Kenny LM, Coombes RC, Oulie I, Contractor KB, Miller M, Spinks TJ, et al. Phase I trial of the positron-emitting Arg-Gly-Asp (RGD) peptide radioligand <sup>18</sup>F-AH11585 in breast cancer patients. *J Nucl Med.* 2008; 49: 879-86.
- Beer AJ, Lorenzen S, Metz S, Herrmann K, Watzlowik P, Wester HJ, et al. Comparison of integrin  $\alpha v \beta 3$  expression and glucose metabolism in primary and metastatic lesions in cancer patients: a PET study using <sup>18</sup>F-galacto-RGD and <sup>18</sup>F-FDG. *J Nucl Med.* 2008; 49: 22-9. doi:10.2967/jnumed.107.045864.
- Wu C, Yue X, Lang L, Kiesewetter DO, Li F, Zhu Z, et al. Longitudinal PET imaging of muscular inflammation using <sup>18</sup>F-DPA-714 and <sup>18</sup>F-Alfatide II and differentiation with tumors. *Theranostics.* 2014; 4: 546-55. doi:10.7150/thno.8159.
- Guo J, Guo N, Lang L, Kiesewetter DO, Xie Q, Li Q, et al. <sup>18</sup>F-alfatide II and <sup>18</sup>F-FDG dual-tracer dynamic PET for parametric, early prediction of tumor response to therapy. *J Nucl Med.* 2014; 55: 154-60. doi:10.2967/jnumed.113.122069.
- Horton MA, Dorey EL, Nesbitt SA, Samanen J, Ali FE, Stadel JM, et al. Modulation of vitronectin receptor-mediated osteoclast adhesion by Arg-Gly-Asp peptide analogs: a structure-function analysis. *J Bone Miner Res.* 1993; 8: 239-47. doi:10.1002/jbmr.5650080215.
- Zheleznyak A, Wadas TJ, Sherman CD, Wilson JM, Kostenuik PJ, Weilbaecher KN, et al. Integrin  $\alpha v \beta 3$  as a PET imaging biomarker for osteoclast number in mouse models of negative and positive osteoclast regulation. *Mol Imaging Biol.* 2012; 14: 500-8. doi:10.1007/s11307-011-0512-4.
- Wadas TJ, Deng H, Sprague JE, Zheleznyak A, Weilbaecher KN, Anderson CJ. Targeting the  $\alpha v \beta 3$  integrin for small-animal PET/CT of osteolytic bone metastases. *J Nucl Med.* 2009; 50: 1873-80. doi:10.2967/jnumed.109.067140.
- Guise TA, Mohammad KS, Clines G, Stebbins EG, Wong DH, Higgins LS, et al. Basic mechanisms responsible for osteolytic and osteoblastic bone metastases. *Clin Cancer Res.* 2006; 12: 6213s-6s. doi:10.1158/1078-0432.CCR-06-1007.
- Rong J, Wang S, Ding Q, Yun M, Zheng Z, Ye S. Comparison of <sup>18</sup>F-FDG PET-CT and bone scintigraphy for detection of bone metastases in breast cancer patients. A meta-analysis. *Surg Oncol.* 2013; 22: 86-91. doi:10.1016/j.suronc.2013.01.002.
- Sprague JE, Kitaura H, Zou W, Ye Y, Achilefu S, Weilbaecher KN, et al. Non-invasive imaging of osteoclasts in parathyroid hormone-induced osteolysis using a <sup>64</sup>Cu-labeled RGD peptide. *J Nucl Med.* 2007; 48: 311-8.
- Suva LJ, Washam C, Nicholas RW, Griffin RJ. Bone metastasis: mechanisms and therapeutic opportunities. *Nat Rev Endocrinol.* 2011; 7: 208-18. doi:10.1038/nrendo.2010.227.
- Glaspy JA, Hawkins R, Hoh CK, Phelps ME. Use of positron emission tomography in oncology. *Oncology (Williston Park).* 1993; 7: 41-6, 9-50; discussion -2, 5.
- Cheng G, Chen W, Chamroonrat W, Torigian DA, Zhuang H, Alavi A. Biopsy versus FDG PET/CT in the initial evaluation of bone marrow involvement in pediatric lymphoma patients. *Eur J Nucl Med Mol Imaging.* 2011; 38: 1469-76. doi:10.1007/s00259-011-1815-z.
- Wang J, Weiss LM, Chang KL, Slovak ML, Gaal K, Forman SJ, et al. Diagnostic utility of bilateral bone marrow examination: significance of morphologic and ancillary technique study in malignancy. *Cancer.* 2002; 94: 1522-31.
- Evangelista L, Panunzio A, Polverosi R, Ferretti A, Chondrogiannis S, Pomerri F, et al. Early bone marrow metastasis detection: the additional value of FDG-PET/CT vs. CT imaging. *Biomed Pharmacother.* 2012; 66: 448-53. doi:10.1016/j.biopha.2012.06.004.
- Liapis H, Flath A, Kitazawa S. Integrin alpha V beta 3 expression by bone-residing breast cancer metastases. *Diagn Mol Pathol.* 1996; 5: 127-35.
- Hetzel M, Arslanemir C, Konig HH, Buck AK, Nussle K, Glatting G, et al. F-18 NaF PET for detection of bone metastases in lung cancer: accuracy, cost-effectiveness, and impact on patient management. *J Bone Miner Res.* 2003; 18: 2206-14. doi:10.1359/jbmr.2003.18.12.2206.
- Miao W, Zheng S, Dai H, Wang F, Jin X, Zhu Z, et al. Comparison of <sup>99m</sup>Tc-3PRGD2 integrin receptor imaging with <sup>99m</sup>Tc-MDP bone scan in diagnosis of bone metastasis in patients with lung cancer: a multicenter study. *PLoS One.* 2014; 9: e111221. doi:10.1371/journal.pone.0111221.